December, 2014

Applications of Discrete Element Method in Modeling of Grain Postharvest Operations

Josephine M. Boac, *Kansas State University*
R. P. Kingsly Ambrose, *Kansas State University*
Mark E. Casada, *United States Department of Agriculture*
Ronaldo G. Maghirang, *Kansas State University*
Dirk E. Maier, *Kansas State University*

Food Eng Rev (2014) 6:128–149
DOI 10.1007/s12393-014-9090-y

REVIEW ARTICLE

Applications of Discrete Element Method in Modeling of Grain Postharvest Operations

Josephine M. Boac · R. P. Kingsly Ambrose · Mark E. Casada · Ronaldo G. Maghirang · Dirk E. Maier

Received: 8 March 2014 / Accepted: 24 July 2014 / Published online: 6 August 2014

Abstract Grain kernels are finite and discrete materials. Although flowing grain can behave like a continuum fluid at times, the discontinuous behavior exhibited by grain kernels cannot be simulated solely with conventional continuum-based computer modeling such as finite-element or finite-difference methods. The discrete element method (DEM) is a proven numerical method that can model discrete particles like grain kernels by tracking the motion of individual particles. DEM has been used extensively in the field of rock mechanics. Its application is gaining popularity in grain postharvest operations, but it has not been applied widely. This paper reviews existing applications of DEM in grain postharvest operations. Published literature that uses DEM to simulate postharvest processing is reviewed, as are applications in handling and processing of grain such as soybean, corn, wheat, rice, rapeseed, and the grain coproduct distillers dried grains with solubles (DDGS). Simulations of grain drying that involve particles in both free-flowing and confined-flow conditions are also included. Review of the existing literature indicates that DEM is a promising approach in the study of the behavior of deformable soft particulates such as grain and coproducts, and it could benefit from the development of improved particle models for these complex-shaped particles.

J. M. Boac · R. P. K. Ambrose (✉) · D. E. Maier
Department of Grain Science and Industry, Kansas State University, 312 Shellenberger Hall, Manhattan, KS, USA
e-mail: kingsly@ksu.edu

M. E. Casada
Engineering and Wind Erosion Research Unit, USDA-ARS Center for Grain and Animal Health Research, Manhattan, KS, USA

R. G. Maghirang
Department of Biological and Agricultural Engineering, Kansas State University, Manhattan, KS, USA

Keywords Discrete element method · Grain handling · Grain processing · Free-flowing grain · Confined grain

Introduction

Grain kernels are considered finite and discrete materials. At times, flowing grain can behave like a continuum fluid or a collection of individual interacting particles depending, in large part, on the energy imparted to the grain kernels [21]. Granular materials such as cereal grains that exhibit discontinuous behavior cannot be simulated solely using conventional continuum-based modeling techniques such as finite-element or finite-difference methods. Examples of processes dominated by discontinuum behavior include flow of bulk solids in hoppers, feeders, chutes, screens, crushers, ball mills, mixers, and conveyor systems. Micromechanical behavior of particular media, stability of underground mine openings, stability of rock slopes, and mineral processing are other solids handling or processing examples in which continuum theory may be inapplicable [24].

Williams et al. [100] described the discrete element method (DEM) to numerically solve problems involving discrete elements like grain kernels. The DEM belongs to a family of numerical modeling techniques designed to solve problems in engineering and applied science that display gross discontinuous behavior [24, 41, 42]. DEM can analyze multiple, interacting, deformable, discontinuous, or fractured bodies undergoing rotations and large displacements. The basic assumption in DEM is that every discrete element has distinct boundaries that physically separate it

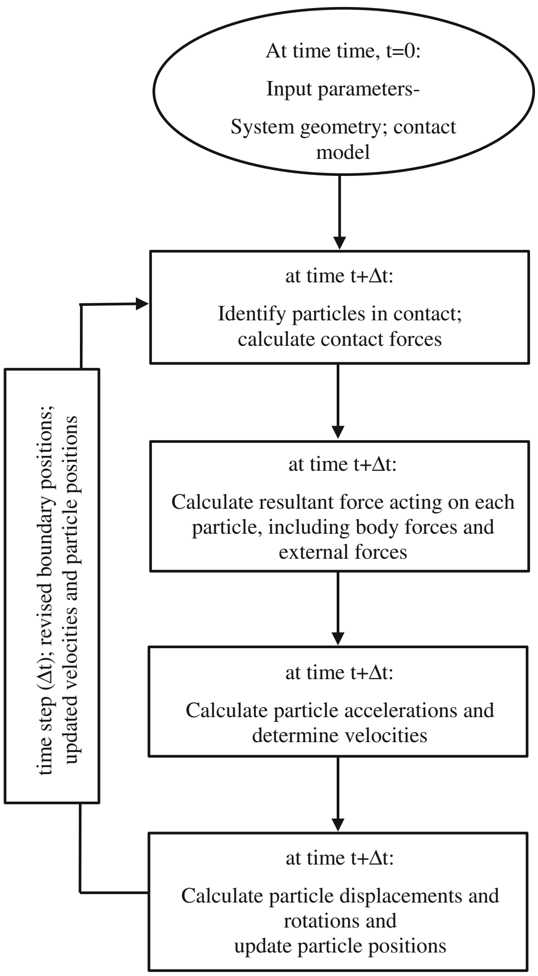

Fig. 1 Overall calculation procedure involved in DEM simulation (adapted from O'Sullivan 2011)

from every other element in the analysis. Basic equations of elasticity are written under an inertial frame and then transferred to a non-inertial frame, which is translating and rotating. This is performed so that to an observer in the non-inertial frame, i.e., the new frame, the object exhibits no mean translation or rotation. The deformation can then be decoupled from the mean motion and written as the sum of the bodies' normal modes, which in turn gives a newly derived set of decoupled modal equations. These equations are applied on an element-by-element basis, and the elements communicate through boundary forces. The decoupled equations are then solved by an explicit central difference scheme, and the final solution is obtained by means of modal superposition [100].

Cundall and Strack [20], who were the first to publish this technique, defined DEM as a numerical model capable of describing the mechanical behavior of assemblies of discs and spheres. The model is based on an explicitly numerical scheme in which the particle interaction is monitored at each contact and the particle motion is modeled particle by particle. Figure 1 illustrates a schematic overview of the sequence of calculations involved in DEM simulation using the central difference, distinct element method proposed by Cundall and Strack [20]. In DEM modeling, particle interaction is treated as a dynamic process, which assumes that equilibrium states develop whenever internal forces in the system balance [84]. Contact forces and displacements of a stressed particle assembly are obtained by tracking the motion of individual particles. Motion results from disturbances that propagate through the assembly. The mechanical behavior of the system is described by the motion of each particle and the force and moment acting at each contact. Zhu et al. [103] also mentioned that DEM simulations can provide dynamic information, such as trajectories of, and transient forces acting on, individual particles, which is extremely difficult or impossible to obtain by physical experimentation at this stage of development. Thus, DEM has been used increasingly to study the particle mechanics in solids handling and processing applications. A complete description of the DEM can be found in Cundall [18], Cundall and Hart [19], Hart et al. [36], and Williams et al. [100].

Discrete element method (DEM) application is gaining popularity in postharvest processing of grain and food products because of its close characterization of actual conditions in predicting various processes. Unlike the field of mining and the chemical industry, however, DEM is not being widely applied because of various particle property issues arising from the biological origins of grain and food products. The objective of this paper was to review existing published research that used DEM as the numerical modeling technique in postharvest grain handling and processing. The scope of this paper is limited to DEM applications on grain and its coproducts.

Theoretical Background of DEM

Approaches in DEM Modeling

Two types of DEM techniques are most common: hard-sphere and soft-sphere approaches. These approaches are differentiated by how the deformation during collision or contact is represented. The hard-sphere approach does not allow deformation or interpenetration during impact [40], whereas the soft-sphere approach does [71, 72, 103]. The hard-sphere approach is at the basis of the collisional or event-driven (ED) models. The ED models are also categorized as non-smooth DEM, which models the shocks between particles by means of shock laws with restitution coefficient [30]. The strategy with ED models is to start with equations governing momentum exchange, which contrasts with the soft-sphere approach that solve the equations governing the linear and angular motion of the colliding or contacting particles [72]. With the hard-sphere approach, the time step interval for the numerical solution varies with the time between each collision. In contrast, the soft-sphere approach uses a constant time step interval in the solutions.

The ED method is limited to circular or spherical particles, takes into account collisions or shocks between two colliding particles only, and does not consider multiple contacts [30]. A sequence of instantaneous collisions is processed, one collision at a time, and the forces between particles often are not explicitly considered [103]; therefore, the hard-sphere approach or the ED method is typically most useful in rapid granular flow simulations, where the granular material is not dense because it has been partially or completely fluidized [72]. The hard-sphere approach is computationally cheap and, therefore, may be preferred for non-dense flow. However, Delaney et al. [22] argued that this approach, although computationally faster, falls short in describing the details of the dense material's response involving multiple simultaneous contacts.

Fortin et al. [30] developed an improved non-smooth DEM based on non-smooth contact dynamics (NSCD). The NSCD method models the contact between particles with the Coulomb unilateral contact law with dry friction and takes into account multiple contacts and shocks between particles [50]. Fortin et al. [30] improved the NSCD by overcoming the difficulties that arise in using the dry friction modeled by Coulomb's law, which is typically non-associated (i.e., during the contact, the sliding vector is not normal to the friction cone). They used bi-potential theory, which leads to a fast predictor–corrector scheme involving just an orthogonal projection onto the friction cone and allows using a convergence criterion based on an error estimator in the constitutive law. According to O'Sullivan [72], the contact dynamics method is not strictly under the hard- or soft-sphere approaches; they are sometimes referred to as rigid body dynamics.

Cundall and Strack [20] originally developed the soft-sphere method, which was the first discrete numerical modeling technique published in the literature. Particles in the soft-sphere approach are also rigid but they are permitted to overlap at the contact points as a representation of the deformation that occurs at the contacts [71, 72, 103]. These deformations are used to calculate elastic, plastic, and frictional forces between particles; the motion of particles is described by Newton's laws of motion. The major advantage of soft-sphere models is that they are capable of handling multiple particle contacts, which is important when modeling quasi-static systems [103].

Advantages of the soft-sphere approach in modeling dense-phase bulk granular materials were also highlighted by Campbell [7]. He emphasized that dense granular materials (as opposed to those fluidized or in dilute phase) in bulk are soft because their sound speed is approximately 50 times slower than those of their constituent solid materials, and the bulk has an apparent elastic modulus more than three orders of magnitude smaller than its constituent solid. He added that dense systems interact by force chains (which are quasi-liner structures that support the bulk of the internal stress within the material) and transmit force along the chain by elastically deforming the interparticle contacts. Modeling such systems as rigid spheres and any other model would miss essential physics [7]. He also mentioned that particle surface friction is essential to modeling dense systems because removing it can cause transition between an elastic and inertial flow regime. Surface friction is important to the strength of the force chains, and force chains are vital to the elastic flow regimes; thus, friction is also essential physics required in the simulation to avoid erroneous behavior.

The soft-sphere approach, with the advantages listed above for describing the bulk material physics, is most commonly used in the grain and food processing industries. Thus, soft-sphere DEM modeling is the focus of this review.

Governing Equations of Motion

In soft-sphere DEM, contact forces and displacements of the particle assembly are computed by tracking the motion of each individual particle using an explicit numerical scheme and a very small time step [20]. The process uses Newton's laws of motion that gives the relationship between the particle motion and forces acting on each particle. Translational and rotational motions of a particle are defined as [78]:

$$m_i \frac{\mathrm{d}v_i}{\mathrm{d}t} = \sum_j \left(F_{n_{ij}} + F_{t_{ij}}\right) + m_i g \quad (1)$$

$$I_i \frac{\mathrm{d}\omega_i}{\mathrm{d}t} = \sum_j \left(R_i \times F_{t_{ij}}\right) + \tau_{ij} \quad (2)$$

where m_i, R_i, v_i, ω_i, and I_i are the mass, radius, linear velocity, angular velocity, and moment of inertia of particle i, respectively; $F_{n_{ij}}$, $F_{t_{ij}}$, and τ_{ij} are the normal force, tangential force, and torque acting on particles i and j at contact points, respectively; g is the acceleration due to gravity; and t is the time.

Modeling of Contact Forces

Force–displacement laws at contact points can be represented by different contact models. The wide range of contact models and their corresponding equations is not discussed in detail in this review. Zhu et al. [103] summarize various contact force models as well as non-contact

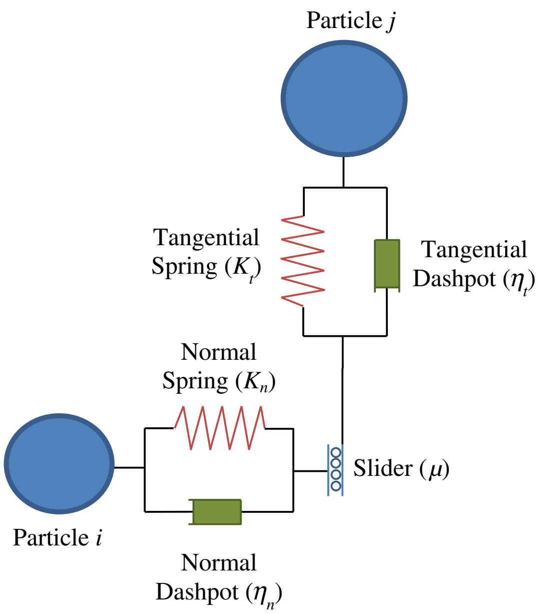

Fig. 2 Elastic contact model with viscous damping and frictional slider in the tangential direction

force models used in discrete particle simulations. O'Sullivan [72] also gives detailed discussions of contact models in her book.

The simplest contact model commonly used is the linear spring-dashpot model [20], in which the spring stiffness is assumed to be constant [69]. An improvement to the linear contact model employs the Hertz theory to obtain the force deformation relation for the contact (e.g., nonlinear spring-dashpot model). Unlike the linear contact model, the Hertzian contact law considers that normal stiffness varies with the amount of overlap. This approach has been extended to cases in which colliding bodies tend to deform (constrained plastic deformation). Numerical models of interaction at the contact involve the force–deformation equation, which is augmented with a damping term to reflect dissipation in the contact area.

One model to represent the force–displacement laws at the contacts is the Hertz-Mindlin contact model [25, 26, 67, 68, 87]. This nonlinear model features both the accuracy and simplicity derived from combining the Hertz theory in the normal direction and the Mindlin model in the tangential direction [78, 87]. Forces on the particles at contact points include contact force and viscous contact damping force [102]. These forces were calculated by assuming the presence of elastic springs and dashpots in the normal (n) and tangential (t) directions (Fig. 2).

The normal force, F_n, is given as follows [78, 87]:

$$F_n = -K_n \delta_n^{3/2} - \eta_n \dot{\delta}_n \delta_n^{1/4} \quad (3)$$

where K_n is the normal stiffness coefficient; δ_n is the normal overlap or displacement; $\dot{\delta}_n$ is the normal velocity; and η_n is the normal damping coefficient.

The tangential force, F_t, is governed by the following equation [78, 87]:

$$F_t = -K_t \delta_t - \eta_t \dot{\delta}_t \delta_n^{1/4} \quad (4)$$

where K_t is the tangential stiffness coefficient; δ_t is the tangential overlap; $\dot{\delta}_t$ is the tangential velocity; and η_t is the tangential damping coefficient. The tangential overlap is calculated by [78]:

$$\delta_t = \int v_{\mathrm{rel}}^t \mathrm{d}t \quad (5)$$

where v_{rel}^t is the relative tangential velocity of colliding particles and is defined by [78]:

$$v_{\mathrm{rel}}^t = \left(v_i - v_j\right) \cdot s + \omega_i R_i + \omega_j R_j \quad (6)$$

where s is the tangential decomposition of the unit vector connecting the center of the particle.

In addition, a tangential force is limited by Coulomb friction ($\mu_s F_n$), where μ_s is the coefficient of static friction. When necessary, rolling friction can be accounted for by applying a torque to contacting surfaces. The rolling friction torque, τ_i, is given by [78, 83]:

$$\tau_i = -\mu_r F_n R_0 \omega_0 \quad (7)$$

where μ_r is the coefficient of rolling friction, R_0 is the distance of the contact point from the center of the mass, and ω_0 is the unit angular velocity vector of the object at the contact point [25, 57, 78, 83, 87].

Stiffness and Damping Coefficient

After modeling the contact forces, the next step is to determine the values of stiffness, K, damping coefficient, η, and friction coefficient, μ. The friction coefficient is measurable and considered a parameter obtained empirically. The damping coefficient can be computed from stiffness. Thus, the stiffness is the parameter that must be determined first and can be computed by Hertzian contact theory when the physical properties such as Young's modulus and Poisson ration are known [87].

Following the Hertz-Mindlin contact model above, the normal stiffness and normal damping coefficients are [78, 87]

$$K_n = \frac{4}{3} E^* \sqrt{R^*} \quad (8)$$

$$\eta_n = \frac{\ln e}{\sqrt{\ln^2 e + \pi^2}} \sqrt{m^* K_n} \quad (9)$$

where E^* is the equivalent Young's modulus, R^* is the equivalent radius, m^* is the equivalent mass, and e is the coefficient of restitution. Equivalent properties (R^*, m^*, and E^*) during collision of particles with different materials such as particles i and j are defined as [25, 83]

$$R^* = \left(\frac{1}{R_i} + \frac{1}{R_j}\right)^{-1} \quad (10)$$

$$E^* = \left(\frac{1 - v_i^2}{E_i} + \frac{1 - v_j^2}{E_j}\right)^{-1} \quad (11)$$

$$m^* = \left(\frac{1}{m_i} + \frac{1}{m_j}\right)^{-1} \quad (12)$$

where v is the Poisson's ratio [25, 83]. Similarly, for a collision of a sphere i with a wall j, the same relations apply for Young's modulus E^*, whereas $R^* = R_i$ and $m^* = m_i$.

Tangential stiffness and tangential damping coefficients are defined as follows [78, 83, 87]:

$$K_t = 8G^* \sqrt{R^* \delta_n} \quad (13)$$

$$\eta_t = \frac{\ln e}{\sqrt{\ln^2 e + \pi^2}} \sqrt{m^* K_t} \quad (14)$$

where G^* is the equivalent shear modulus defined by [57]

$$G^* = \left(\frac{2 - v_i}{G_i} + \frac{2 - v_j}{G_j}\right)^{-1} \quad (15)$$

G_i and G_j are shear moduli of particles i and j, respectively.

Critical Time Step

For dynamic processes, important factors to consider are the propagation of elastic waves across the particles, the time for load transfer from one particle to adjacent contacting particles, and the energy transmission across a system that should not be faster than in nature [57]. In the nonlinear contact model (e.g., Hertzian), the critical time increment or critical time step cannot be calculated beforehand, unlike the linear contact model in which the critical time step is related to the ratio of contact stiffness to particle density. Miller and Pursey [66], however, showed that Rayleigh waves or surface waves account for 67 % of the radiated energy, whereas dilational or pressure waves and distortional or shear waves are 7 % and 26 %, respectively, of the radiated energy. Thus, it is assumed that all of the energy is transferred by the Rayleigh waves because the speed difference between the Rayleigh wave and the distortional wave is small, and the energy transferred by the dilational wave is negligible [57]. Moreover, the average time of arrival of the Rayleigh wave at any contact remains the same irrespective of the contact point location. For simplicity, the critical time step is based on the average particle size, and a fraction of this is used in the simulations [57, 83]. The critical time step is given by the following equation [57, 83]

$$t_c = \frac{\pi \bar{R}}{\beta} \sqrt{\frac{\rho_p}{G}} \quad (16)$$

where $\bar{R}$ is the average particle radius, ρ_p is the particle density, G is the particle shear modulus, and β can be approximated by [57]

$$\beta = 0.8766 + 0.163\, v \quad (17)$$

A major concern in using the DEM is the computational time because of the calculation of particle interactions and spatial movement at very small time steps. Boukouvala et al. [6] developed the discrete element-reduced-order modeling (DE-ROM) approach to reduce computational time. The authors used principal component analysis (PCA) based on the data decomposition approach for discrete simulation and validated the new approach by studying a mixing process. Although this approach is encouraging, it requires data preprocessing to identify the optimal discretization based on the geometry and the state variable variability. This recently published work has not been adapted in grain postharvest operation modeling.

Particle Models: Grain and its Coproducts

The choice of shape representation for modeling particles is critical to the accuracy of real particle behavior during simulation, contact detection, and computation for contact forces determination [28, 39]. The earliest particle models were two-dimensional (2D) and of circular [20] or polygonal shapes [92]. Later developments extended representations to three-dimensional (3D) shapes, using spheres [17], polyhedra [18, 38], ellipses [86], ellipsoids [59], superquadric functions [39, 99], multi-element axisymmetrical non-spherical particles [28], and bonded particles [65, 74]. Although contact detection and computation time are very important, the critical objective in DEM modeling is accurate simulation of the behavior of an assembly of real particles [28]. Favier et al. [28] also mentioned that the influence of particle shape on predicted behavior is less documented than the relationship between shape and the efficiency of contact detection, with the exception of particle models that used polyhedral shapes [31, 36]. In the following sections, the particle models developed and used for predicting handling and processing behavior of cereal grains, oilseeds, and their coproducts are explored and summarized in Table 1.

Soybeans

Soybean is one of the major oilseeds produced around the world. Like any other agricultural grain, the

Table 1 Summary of particle models used for grains and coproducts

Grain type	Particle model	References
Soybeans	2D single circular disc model	Li et al. [55]
	3D four-sphere model	LoCurto et al. [60], Vu-Quoc et al. [91]
	3D single-sphere model	Boac et al. [4, 5]
Corn	2D two-disc clump model	Coetzee and Els [13–15]
	3D four-sphere model	Chung and Ooi [8–10]
	3D six-sphere model	González-Montellano et al. [32–34]
Wheat	2D single circular disc model	Iroba et al. [46, 47], Mellman et al. [64]
	2D five-disc ellipsoidal clump model	Weigler et al. [94]
	3D three-sphere model	Keppler et al. [53]
	Comparisons: 3D single-sphere model, 3D four-sphere model, and 3D eight-sphere model	Sarnavi et al. [82]
Rice	2D single circular disc model	Sakaguchi et al. [81]
	3D eleven-sphere ellipsoidal model	Markauskas and Kačianauskas [62]
	3D seven-sphere ellipsoidal model	Jiang and Qiu [51]
	3D spheroid model	Li et al. [58]
Rapeseed	2D single circular disc model	Molenda et al. [70]
	3D single-sphere model	Raji and Favier [76, 77]
	3D single-sphere model	Wojtkowski et al. [101]
	3D single-sphere model	Wiącek and Molenda [97]
	3D single-sphere model	Parafiniuk et al. [73]
DDGS	3D single-sphere model	Clementson [12]

physicochemical properties of soybeans and their products depend on the place of origin and processing methods. Soybean-handling systems and processing operations have been simulated for the past 20 years in an effort to optimize processes. LoCurto et al. [60] used a particle model for soybeans consisting of a cluster of four spheres of equal radius, with centers lying on a plane. This was similar to Favier et al.'s [28] representation of non-spherical particles comprising overlapping spheres with centers fixed in a position relative to each other along the major axis of the particle's symmetry. The 3D four-sphere particle model was used to simulate the behavior of a single soybean kernel bouncing in aluminum, glass, and acrylic surfaces to measure the coefficient of restitution. The simulations predicted the coefficient of restitution with reasonable accuracy. Vu-Quoc et al. [91] created a soybean particle model based on the multi-sphere method developed by Favier et al. [28] to predict the dry granular flow of soybean in a chute.

Soybean kernels resemble a sphere with high average sphericity values of above 0.8 [48]; thus, to reduce computation times, single spheres were used by most researchers to simulate bulk soybean characteristics. Li et al. [55] simulated the separation of soybeans and mustard seeds in a sieve using 2D DEM and modeling soybeans as circular discs. They used a linear spring model and modified their codes by conducting trial runs to select the appropriate time step for the simulations. Both kernels (soybeans and mustard seeds) were assumed to have uniform particle size. The screen wire was also modeled in DEM using a group of circular particles that had the properties of the screen wires, and these particles were vibrated to simulate the movement of a mechanically agitated screen. The authors found that the two spherical particle models representing soybeans and mustard seeds in a screening process were adequate and that the DEM simulation can provide the critical feeding rate for the most effective screening operation. Boac et al. [4] used a single-sphere particle model to simulate bulk soybean property testing using EDEM (DEM Solutions, Ltd., Edinburgh, UK), a commercial DEM code. The researchers used a no-slip Hertz-Mindlin contact to simulate and model the bulk density and angle of repose measurement tests. They conducted this simulation to develop a particle model with appropriate parameter combinations of coefficients of restitution, static friction, rolling friction, particle size distribution, and particle shear modulus that best matched the property values available in the literature. The developed soybean particle model was then used to simulate the commingling of two soybean lots, with different intrinsic properties, in a bucket-type grain elevator boot system [5].

Corn

Corn is a cereal grain that is grown widely throughout the world and is a major food grain in Africa and Latin America, with the United States as its largest producer. In the United States, almost 85 % of corn produced is used as livestock feed and as a raw material for industrial products [27]. The design and development of processing and handling equipment for corn is a mature area, but because of the volume of grain handled and the new varieties that are being developed and to mitigate dust issues, particle modeling is being used to improve the design of equipment. Chung and Ooi [8–10] modeled corn kernels using overlapping spheres to match the measured average major, intermediate, and minor dimensions. They used particle flow code (PFC) 3D (Itasca Consulting Group, Inc., Minneapolis, MN), a commercial DEM code, to simulate a confined compression and rod penetration in a dense granular medium [8, 9] and silo discharging [10]. The authors used a four-sphere particle representation for corn because increasing the number of spheres in a single particle leads to additional computational cost [8]. Measured material properties [11] were used for simulation purposes.

Modeling corn particles using overlapping discs called clumps in PFC 2D also has been employed in the development of particle models of Coetzee and Els [13–15]. A clump is a single entity composed of two or more overlapping spheres (in 3D) and discs (in 2D) to form one rigid particle. Internal contact forces between the overlapping spheres or discs are ignored in calculations [61]. Clumps do not break during simulations regardless of the forces acting upon them [29, 49]. Coetzee and Els [13–15] used this 2D clump corn particle model to calibrate material parameters such as the particle internal friction angle using laboratory shear tests and particle stiffness using compression tests. They validated the calibration process by modeling silo discharge and bucket filling. Coetzee et al. [16] extended these studies to DEM modeling of dragline bucket filling using particle models comprising 2–4 overlapping spheres that represent crushed rocks.

The highest number of spheres used to develop a corn particle model was simulated by González-Montellano et al. [32–34]. They modeled corn kernels consisting of six spheres using the multi-spheres method [28] and experimentally derived material property values [35]. The authors indicated that using more than six spheres to construct one corn particle would have slowed their simulation significantly, thus increasing computation time. The friction coefficients of this corn particle model were used to predict the flow patterns of the discharging particles from a silo González-Montellano et al. [32]. Then, they applied this modified corn particle model to study the pressure distributions, bulk density distributions, and flow properties during filling and emptying of silos [33, 34].

Wheat

Wheat is a highly irregularly shaped kernel whose shape representation for simulation purposes is challenging; the presence of a crease makes it difficult to develop a particle with identical spheres. Studies have reported using wheat kernels in 2D to investigate the flow of wheat in a mixed-flow grain dryer [46, 47, 64, 94]. Monosized spherical particles were used to model the grain dryer in 2D using PFC 2D software. Iroba et al. [46] indicated that using multiple spheres would make the simulation time longer, whereas using non-spherical particles would be more difficult to model and would require more advanced algorithms. Because of the disc shape of the 2D particles in the simulation, however, bridging between particles occurred at the bottom discharge device of the grain dryer, which did not happen during experiments. Iroba et al. [46, 47] explained that because the long and ellipsoidal shape of wheat kernels can orient in different directions during discharge, flow can be enhanced and bridging did not occur in the experiment. Spherical particles (discs) tend to form bridges even though orientation is the same in all directions. To overcome bridging of particles during simulation, the fixed part of the discharge device was vibrated. In the subsequent simulations, the authors used non-spherical particles represented by a 2D ellipsoidal clump consisting of five circular elements [94]. The clumps were assumed to have the same material properties as wheat, which were adapted from Markauskas et al. [63]. The DEM model indicated that using non-spherical particles (2D ellipsoidal clumps) can predict the real flow pattern, but disc-shaped particles did not produce the expected dynamic angle of repose that typically formed under the air ducts.

Keppler et al. [53] predicted the velocity distribution of wheat kernels in a mixed-flow dryer with 3D wheat kernels using EDEM software. The wheat particle was represented by a clump of three spheres. Although the particles used in EDEM were slightly bigger than actual particles, the velocity prediction was nearly accurate. To compare the performance of different particle models, Sarnavi et al. [82] simulated 3D wheat kernels using three types of particle models: (1) spherical, (2) 4 spheres, and (3) 8 spheres using the PFC 3D software. They compared the performance of the particle models with two contact models (linear vs. nonlinear) in predicting the angle of internal friction and cohesion of wheat. They found that the single spherical particle model, using both linear and nonlinear contact models, performed better in the simulations than the multi-sphere models. Although different particle models have been used to simulate wheat kernels, the studies clearly demonstrate that 3D particle models have higher accuracy in predicting the bulk behavior of wheat than a 2D approach. The results do not, however, confirm the best number of spheres to use to represent a single wheat kernel. This could be because of the complicated shape of wheat kernels; the number of spheres should be approximated by trials depending on the computation time and prediction accuracy required.

Rice

Rice's ellipsoidal shape is similar to wheat, but the absence of a crease in rice makes it easier to approximate the rice particle shape. A 2D circular disc approach was used by Sakaguchi et al. [81] to model rice kernels in the shaking separation process using their own DEM codes [80]. The authors obtained good agreement between the simulation and experiment with respect to the wave-like behavior of the grain assembly and the macroscopic separation behavior of rice. Markauskas and Kačianauskas [62] modeled rice kernels by creating an ellipsoid using 11 spheres. They compared two rice particle models, with rolling friction coefficients of zero and 0.3, using their own DEM code [52]. These particle models were used to simulate the filling and discharge flow and piling of the kernels. The particle model with rolling friction produced a pile shape that better corresponded to the actual pile. On the other hand, the particle model without rolling friction showed higher particle mobility, resulting in a spread of particles rather than a pile. A 7-sphere particle model was used by Jiang and Qiu [51] to simulate the impact behavior of rice kernels. The rice particle modeled was an ellipsoid with a 3.5-mm half-major axis and a 1.8-mm half-minor axis. The authors implemented this rice model in EDEM software and studied the impact of rice particles on the impact board of an inclined elevator head. Simulations predicted the experimental results with high accuracy up to a certain mass of rice that impacts the board. A 3D rice model was also used by Li et al. [58] to simulate the material motion in an air-and-screen cleaning device. The authors separated rice kernels and straws using a coupled DEM and computational fluid dynamics (CFD) model. The rice grain was represented in EDEM by a spheroid that is 6 mm long with a 1.6 mm radius of rotation. The short straw was represented by a cylinder 30 mm long by 4 mm diameter. These models were used to study the effect of inlet airflow velocity in terms of the longitudinal velocity, vertical height, and cleaning loss of rice kernels and short straws. The coupled CFD–DEM model predicted the air-and-screen cleaning process by describing the movement of particles on the screen surface. Coupling CFD with DEM is a recent advancement in particle modeling that will be useful in the grain processing industry for the prediction of various handling and processing operations.

Rapeseed

Rapeseed is the second leading source of vegetable oil and protein meal in the world next to soybean [88]; thus, its processing and handling optimization is important to the industry. Bulk compressive loading of rapeseeds was modeled by Raji and Favier [76] using a single-sphere particle model. They found a slight difference in the initial particle positions between the experiment and simulation, although strain intervals were calculated at the same porosity values. This was an early attempt to model rapeseeds, and the authors extended the use of this single-sphere particle model to simulate rapeseed, soybean, and palm-kernel for bulk compression [77]. Later, other researchers also modeled rapeseed using a single-sphere particle model to simulate the free fall and impact of rapeseeds against a flat surface [101]. The authors used two different contact models, an elastoplastic contact model for dry seeds by Thornton and Ning [85] and a viscoelastic contact model for wet seeds by Kuwabara and Kono [54]. Parafiniuk et al. [73] simulated rapeseeds as single spheres to predict flow through a horizontal orifice. The experimental mean radii and standard deviation values were used to develop the single-sphere model. The authors used EDEM software and applied the contact models used by Wojtkowski et al. [101] for dry and wet rapeseeds. Parafiniuk et al. [73] concluded that the contact models reproduced experimental results for slow particle flow but needed the improvement of including dissipation for higher particle flow rates. Wiącek and Molenda [97] studied the influence of the moisture content of rapeseeds on the physical properties of grain bedding during uniaxial compression testing using single-sphere particle models. Results indicated that the mechanical response of a granular assembly subjected to uniaxial compression is significantly affected by the moisture content of kernels. Both the simulations and experiments revealed differences in the elasticity and the stress transmission within rapeseed assemblies at various grain moisture contents.

The behavior of rapeseed during a direct shear test was modeled by Molenda et al. [70] using 2D circular discs. They used circular elements with size uniformly distributed between 1.8 and 2.2 mm. Numerical simulations were performed using a non-commercial DEM code [93] to determine the influence of three different levels of standard deviations in the coefficient of interparticle friction to the bulk behavior in a direct shear test. Particle interaction in the normal direction was simulated using a linear viscoelastic model, whereas the tangential direction was expanded to include a frictional element. Variability in the interparticle friction was found to influence markedly the stress–strain characteristic during the initiation of motion, whereas the strength of the assembly (or steady-state value of stress) remained constant.

Grain Coproducts

Grain undergoes different processing methods during conversion into products and coproducts. The particle characteristics of products derived from grain are generally controlled, but particle characteristics are not uniform because the bulk contains particles with different sizes, shapes, and chemical compositions. The challenge in modeling coproduct is in shape representation using spheres. For example, distillers dried grains with solubles (DDGS), a coproduct from corn-to-ethanol processing, which contains a mixture of fiber, starch, and protein components that vary in size and shape. Clementson [12] modeled the flow and segregation of DDGS using single-sphere particle model in EDEM with the Hertz-Mindlin (no-slip) contact model. The geometric mean diameter of actual DDGS ranged from 0.87 to 1.01 mm, but the researchers used bigger particles because small particles required longer simulation time in DEM; the log-normal bimodal distribution of these particles was kept similar to the actual particle size distribution. The author found that the magnitude of changes in discharge rates in the experiments was not the same as in the simulation, and the numerical simulation predicted the same flow patterns as observed during funnel flow but not mass flow experiments. DEM has not been widely used to predict the bulk behavior of coproducts from the grain-based food and feed industry, partially because of the computational load from the higher number of spheres required to obtain accurate shape representation.

Modeling Grain Handling Operations

Bulk behavior of cereal grains, oilseeds, and their products varies based on the quantity, environmental factors, method of processing, and handling equipment used. The grain handling and processing operations that have been modeled using DEM were subdivided into processes dealing with free-flowing grain, such as filling and emptying of silos, and confined grain, such as storage and compression.

Gran Postharvest Operations Modeled or Studied Using DEM

- Free-flowing grain
  - Filling and discharge of silo
  - Bulk behavior during grain conveying
  - Grain cleaning and separation
  - Impacting grain kernels
- Confined grain
  - Silo probing
  - Compression
  - Shear testing
- Grain drying

Table 2 summarizes the model and references associated with these postharvest processing

Modeling Free-Flowing Grain

Filling and Discharge of Silo

Due to the complexity of physical and chemical parameters, hopper flow of grain and grain products usually encounters challenges such as ratholing, arching, and caking. Use of discharge aids in grain-based food and feed industries is a common practice to achieve uniform flow of material from hoppers and silos. DEM is increasingly applied to simulate bulk flow characteristics of grain and products for better bin design and process optimization.

Table 2 Summary of major studies in modeling grain handling processes

Process	Specific model	References
Free-flowing grain	Filling and discharge of silo	González-Montellano et al. [32–34]
		Chung and Ooi [9, 10]
		Coetzee and Els [13]
		Clementson [12]
		Markauskas and Kačianauskas [62]
		Parafiniuk et al. [73]
	Bulk behavior during grain conveying	Coetzee and Els [13, 15]
		Boac et al. [4, 5]
	Grain cleaning and separation	Sakaguchi et al. [81]
		Li et al. [55, 58]
	Impacting grain kernels	Wojtkowski et al. [101]
		Jiang and Qiu [51]
Confined grain	Silo probing	Chung and Ooi [8]
	Compression	Raji and Favier [76, 77]
		Chung and Ooi [8–10]
		Wiącek and Molenda [97]
		Coetzee and Els [13, 14]
	Shear testing	Molenda et al. [70]
		Sarnavi et al. [82]
Combined models (free-flowing and confined)	Grain drying	Iroba et al. [46, 47]
		Mellman et al. [64]
		Keppler et al. [53]
		Weigler et al. [94]

Different grain filling approaches have been used to simulate grain storage systems. Progressive filling is the more common method used in DEM simulation where particles are generated continuously, whereas in *en masse* filling, all particles are generated simultaneously, thus reducing computation time. In *en masse* filling, particles

Table 3 Summary of findings and limitations of published research, research and development needs, and knowledge gaps

Previous research	Research findings and limitations	Research and development needs and knowledge gaps	References
Particle models			
Corn in compression, silo probing, silo filling, and discharge	Used 3D 4-sphere and 6-sphere particle models for corn with the assumption that increasing the number of spheres would further increase computation time	Most appropriate number of spheres for describing a single corn particle was not defined; different particle models have been used—a 4-sphere particle model was used for silo discharge, confined compression, and silo probing, whereas a 6-sphere particle model was used in silo filling and discharge. There is a need to define the most appropriate particle model	Chung and Ooi [8–10]; González-Montellano et al. [32–34]
Wheat in mixed-flow grain dryer	Used 2D single circular disc particle model for wheat with the justification that a 3D multi-sphere particle model increases computation time and 3D non-spherical particle model is difficult to model and an advanced algorithm is needed	A better particle model is needed for wheat to solve the problem of bridging of particles (circular discs) at the bottom of the grain dryer; vibration has been used to resolve the bridging during simulation	Iroba et al. [46, 47]
Wheat in shear testing	Tested 3D particle models for wheat (1-, 4-, and 8-sphere models). The particle model that could be used for shear testing is not definite	A better shape representation is needed to model the complicated shape of a wheat kernel; the number of spheres should be approximated by trials depending on the computation time and prediction accuracy required	Sarnavi et al. [82]
Soybean bulk property tests and soybean commingling	Limitations found with excess computation time related to the number of particles, shape of particles (multiple spheres), and with high particle shear modulus. Computation time requires compromises, which are acceptable in some cases, a problem in other cases, and a unacceptable in still other cases	Need to define complex particle shapes to help solve the complex shape part in relation to computation time	Boac et al. [4, 5]
DDGS flow	Used larger particles to model DDGS; predicted the same flow patterns as the experiments but not the magnitude of changes in discharge rates.	DEM not widely used in grain coproducts; need to resolve the high number of spheres required to obtain accurate shape representation.	Clementson [12]
Modeling elements/knowledge			
Corn flow behavior during discharge	Used 2D clump particle model to predict the flow of corn through a silo; higher prediction accuracy through a larger silo opening (less restricted flow)	Prediction accuracy has to be considered when using 2D models	Coetzee and Els [13]
Rice behavior during shaking process	Used 2D circular disc model to predict the separation of brown and paddy rice; the simulation showed the same wave-like behavior of the grain assembly as in the experiment, but the circular particles moved closer to the lower end of the shaker than in the experiment, which was due to the ease of rotation of the circular elements	The rotational issues of circular elements during simulation when using 2D models has to be solved for better prediction	Sakaguchi et al. [81]
Rice in hopper filling and discharge and piling of grains	Tested particle models with and without rolling friction; importance of rolling friction in simulating the angle of repose of a pile of grain	Need to establish the appropriate rolling friction to employ in simulating a specific grain type	Markauskas and Kačianauskas [62]
Rice impact on a surface	DEM was able to predict the effect of particle mass and normal contact force between particles and surface during impact	Further research on the factors that affect the retention and the slippage of a particle after impacting a surface has to be carried out	Jiang and Qiu [51]
Rapeseed flow through a horizontal orifice	Contact models reproduced experimental results for slow particle flow but needed improvement for higher particle flow rates	Further research that take into account the dissipation of energy for particles with high flow rates during flow through a horizontal orifice	Parafiniuk et al. [73]

Table 3 continued

Previous research	Research findings and limitations	Research and development needs and knowledge gaps	References
Rapeseed in compression	Moisture content significantly affected the properties of grain bedding during compression	Application of this model for predicting compression behavior of other common cereals and grains	Wiącek and Molenda [97]
Rapeseed in shear testing	Degree of variation in interparticle friction did not influence the final value of shear strength at steady-state flow, but markedly influenced the shear path (or shear–strain characteristics) at the initiation of motion	Application of this model for predicting shear testing of other common cereals and grains	Molenda et al. [70]
Particle flow behavior during silo filling	Tested three different coefficients of interparticle and particle–wall friction; high interparticle friction led to low bulk densities after the silo filling, which agreed with results in simulated bulk density tests	Need to establish the right interparticle and particle–wall friction coefficients for other grain types and surfaces to be used in future simulation	González-Montellano et al. [32]; Boac et al.'s [4]
Modeling methods			
Rice and straw separation in air-and-screen cleaning device	Use of coupled CFD–DEM to study the separation process for rice and straw	Further use in modeling other postharvest processes; another application could be on design improvement of combine harvesters in processes that involve predicting the particle movement in air	Li et al. [58]
Bin pressures	Major concern when using DEM to study bin pressures is that it assumes rigid silo walls in the simulations, resulting in overprediction of the horizontal distribution of normal pressure at the central positions on the walls	Need to explore the use of hybrid models combining DEM and FEM; DEM can be used to accurately simulate the dynamic behavior of the grain itself, and FEM can be used to model flexible walls of the grain dryer	González-Montellano et al. [35]
Mixed-flow grain dryer	DEM can adequately predict the main features of particle flow and air flow as affected by design elements and air duct arrangements. Particles at the near-wall region had lower particle velocity, whereas the central region had high particle velocity, thus resulting in different residence times and affecting overall dryer capacity and drying efficiency	Further studies needed to improve the design of MFDs; coupled CFD–DEM may be explored further to optimize MFD designs	Iroba et al. [46, 47]; Mellman et al. [64]; Keppler et al. [53]; Weigler et al. [94]
	Grains flowing at lower velocities may be over-dried, and those moving at high velocities may be under-dried		

are allowed to fall under gravity until a static equilibrium is reached. González-Montellano et al. [33] used the *en masse* filling approach for glass beads and corn kernels filling in a silo. Particles were deposited rapidly on top of each other, leading to many particles being trapped by the others without having dissipated their initial energy. During emptying, the movement of the material diluted these effects, and the observed pressures were similar to the expected pattern [33]. If the *en masse* method is used in simulations, prediction errors should be taken into account when studying pressures during filling of silos (Table 3).

González-Montellano et al. [34] improved their simulations by using a modified particle model for corn [32] and the progressive method of filling a silo [33] from their previous work. Results highlighted a difference in the vertical distributions of pressure between corn and glass beads. During both filling and discharge, the peak pressure at the silo–hopper transition was much higher for corn than for glass beads. Pressure values also fluctuated less for corn. For horizontal pressure distribution during filling and at any time during the discharge of corn, maximum horizontal pressure was in the central region of the silo walls and then slowly decreased toward the corners. This result was the same for glass beads, except that the distributions were less stable over time. In both models, the velocity profile at the center was greater than at the walls. For corn, the distribution of the bulk density in the vertical section was not as random as with glass beads. These researchers demonstrated DEM's usefulness in studying the behavior of granular materials in silos and hoppers and the degree of detailed information that could be obtained from simulations.

Chung and Ooi [10] simulated silo discharge by emptying corn through a circular orifice of a flat-bottom silo unloading onto a flat surface. Although the purpose of the study was to examine the influence of gravity on a granular solid, the terrestrial aspects of experiments closely simulated earth-bound processes using DEM. DEM simulation showed that the mass flow rate decreases as gravity decreases, with a corresponding increase in discharge time. The simulation also correlated with Beverloo's relationship that the mass flow rate is proportional to the square root of the gravitational force. In addition to corn discharge parameters, DEM also predicted reasonably the angle of repose of corn discharged from the silo [10].

Mass flow rate and size of hopper outlet opening influence discharge of granular materials. Coetzee and Els [13] studied the discharge of corn kernels from a glass rectangular silo in two dimensions using PFC 2D. Two silo openings were used in this study. The authors found that the corn particles modeled as clumps composed of two discs could reasonably predict the flow patterns observed during experiments. The results indicated that a 2D clump particle model had higher accuracy in predicting the flow of corn through a larger silo opening where the flow was less restricted. Accuracy of DEM simulations depends on the particle models and the particle parameter values used in the simulations. In this study, the two-disc particle model could have influenced the prediction accuracy.

Monitoring the density of material that flows from hoppers or bins is one method used to evaluate segregation. Clementson [12] used DEM to predict the bulk density of DDGS particles during funnel flow and mass flow from hoppers. The hopper half angles used were 33° for the mass flow and 65° for funnel flow. DEM predicted a funnel flow for DDGS that was observed during experiments. The results reported by Clementson [12] supported the hypothesis that the heterogeneity of DDGS does not facilitate true mass flow, irrespective of the hopper design.

Discrete element method (DEM) can be used to predict bulk density after filling a silo in addition to flow pattern and discharge rate. González-Montellano et al. [32] used corn kernels and glass beads in EDEM simulations to model silo filling and discharge. For corn, three successive DEM models were tested to identify the coefficients of interparticle and particle–wall friction. High interparticle friction led to low bulk densities after the silo filling, which agreed with Boac et al.'s [4] results in simulated bulk density tests. High interparticle friction also increased the discharge time. For glass beads, the velocity profile was qualitatively similar to corn but showed a more fluctuating velocity profile. This result may be explained by the development of crystalline packing configurations when single-sphere particles were used [9, 32]. For discharge rates, results for the glass beads showed wider fluctuation than those for corn kernels, which was a consequence of the relatively larger ratio between particle size and silo opening used for glass beads (0.24) than for corn (0.17).

An axisymmetric multi-sphere approach is a recent development that could be used to develop particle models for irregularly shaped cereal grains. Markauskas and Kačianauskas [62] used this approach to simulate the filling and discharge of rice from a small-plane wedge-shaped hopper with a rectangular orifice. The authors simulated the angle of repose of the pile of rice after its discharge from the hopper and modeled friction effects on the flow of rice through an orifice. To model the friction effects, two rice particle models, with and without rolling friction, were used. The researchers found that rolling friction must be taken into account to avoid artificial local rotation of particles when using axisymmetric multi-sphere particle models to represent elongated, irregularly shaped particles. Numerical results provided quantitative evidence of increased rolling friction owing to geometric deviations of the particle shape from the axisymmetric geometry. Simulations with zero rolling friction in the model resulted in a lower angle of repose and discharge time compared with the experimental values. The authors also investigated the rotational energy of particles inside the hopper using both models [62]. The rolling friction practically suppressed local spin, whereas the perpendicular rotation occurred because of the collective particle arrangement. The authors showed the effects of rolling friction to rotational behavior of the particles and that neglecting the rolling friction led to increased capability of particles to rotate by falling on the pile.

The effect of moisture content on the mass flow rate of rapeseed from a silo was modeled by Parafiniuk et al. [73], who verified the applicability of the elastoplastic model for dry seeds and the viscoelastic model for wet seeds adapted from Wojtkowski et al. [101] in DEM simulations. Simulation results revealed that the proposed contact models reproduced the experimental results for slower rate of particle flow. At higher flow rates (or larger openings), however, the dissipation of energy led to higher noise in the force simulated on the silo bottom than indicated by the experimental results. This discrepancy was higher in simulations where the elastoplastic contact model (for dry seeds) was used. In DEM simulations, mass flow rates of dry and wet seeds did not differ if the mass flow rates were calculated as a sum of masses of particles falling into the receiving container per time unit, but differences in the mass flow rates of dry and wet rapeseeds were observed if calculated using the sum of vertical forces exerted by particles on walls and floor of receiving container. The authors did not include cohesion parameters in particle models, which resulted in the differences between predictions and experimental results.

The major concern when using DEM to study bin pressures is that it assumes rigid silo walls in the simulations of González-Montellano et al. [34]. This results in overprediction of the horizontal distribution of normal pressure at the central positions on the walls. González-Montellano et al. [34], after continued efforts to simulate grain bins using DEM, recommended that hybrid models combine DEM and the finite-element method (FEM) to compensate for DEM's limitations. DEM allows a more accurate simulation of the dynamic behavior of the granular material itself, and FEM will allow flexible walls to be included, thus yielding a complete model.

Bulk Behavior During Grain Conveying

Shear zone theory was applied by Coetzee and Els [13] to simulate bucket filling using DEM. The authors used a rig geometry that resembled a dragline bucket, which was pulled in the drag direction by a set of ropes but with freedom of motion in all other directions, based on the shear zone theory developed by Rowlands [79]. DEM can accurately predict the filling process of a bucket or scoop, the force acting on the bucket, and the fill rate. During the experiments, the flow regimes as predicted by the shear zone theory [79] were also observed. DEM predicted these different flow zones [13–15], and the authors recommended that knowledge of the flow zones can be used to optimize buckets in terms of fill rate, bucket force, and bucket wear.

Grain commingling is an unintentional introduction of a different grain type during typical handling operations that directly reduces the level of purity in grain that enters an elevator facility. Three approaches address commingling during grain handling: (1) ignore it, (2) identity-preserve (IP) the grain in dedicated containers, and (3) segregate or handle the IP grain in non-dedicated facilities. Due to limited scientific data on grain commingling in normal handling operations, it is not possible to predict the level of purity that could be achieved with the third, less expensive approach [3]. Boac et al. [5] simulated grain commingling in a pilot-scale grain elevator boot using DEM models and evaluated the trade-offs of computational speed versus accuracy for 3D and quasi-2D boot models. Experimental data from the pilot-scale bucket elevator showed that the average cumulative commingling was comparable to the values for full-size bucket elevator legs. To avoid overprediction, the 3D model was refined to account for the sudden surge of particles during entry and corrected for the effective dynamic gap between the bucket cups and the boot wall. Comparison of predicted average commingling of five quasi-2D boot models with reduced control volumes showed that the quasi-2D (5.6 times the particle diameter) model provided the best option in terms of computation time; it reduced computation time by 72–74 % compared with the 3D model. Results of this study are being applied to study the commingling of infested and sound kernels (wheat and corn) in bucket elevator boot systems.

Grain Cleaning and Separation

The macroscopic behavior of paddy and brown rice during shaking separation was modeled by Sakaguchi et al. [81] on an oscillating inclined separation plate using a 2D DEM model. The grain kernels were represented as circular elements using the model developed by Sakaguchi et al. [80]. In the DEM simulation, the indents on the separation plate were modeled using virtual walls. Particle exit from an indent was modeled as removal of a virtual wall when the particle–wall contact exceeded a threshold value. There was a good agreement between the results of the simulation and the experiment in terms of the macroscopic separation behavior of the rice. The experimental observations such as segregation caused by upward movement of paddy rice relative to brown rice and the shearing of the grain bed to accumulate paddy rice near the lower end of the shaker box were also predicted by the DEM simulation. The time required to achieve maximum separation of brown and paddy rice was the same in both experiment and simulation. In the simulation, the circular particles moved closer to the lower end of the shaker than in the experiment, which was due to the ease of rotation of the circular elements. However, the simulation showed the same wave-like behavior of the grain assembly as in the experiment. The authors concluded that a simple DEM model using 2D circular particles and virtual walls was effective and can be done with reasonable computation times. The model will allow further investigation of the separation mechanism and exploration of the effects of different physical and process parameters on the efficiency of grain separation in shaking separators.

Separation mechanism of grain kernels on sieves is a dynamic process that requires consideration of various particle parameters such as size, shape, density, loading rate, and other factors. Li et al. [55] used a 2D transient model to calculate the motion of discrete soybean and mustard seed particles on sieves using DEM. The authors studied the influence of particle bed depth on undersize particle segregation in an inclined vibrating screen. In the DEM simulation, the sieving screen was modeled to be made of vibrating circular particles (smaller than the kernels) with properties of the sieving wires. The numerical simulation indicated that at a particle bed depth of about 5 times the size of the large particles and 12 times the size of the screen apertures, most undersize particles segregated to the screen surface. The undersize particles also passed through the apertures within about 40 % of the sieve length at the front section of the screen. For this particle bed depth, the screen length was long enough to ensure the highest screening efficiency, 100 % separation, which means no undersize particle passed over and joined the overflow of large particles at the end of the screen. The authors concluded that for a screening system involving granular materials, the critical feeding rate needed to achieve the most efficient screening process can be determined using DEM simulation. Li et al. [56] extended this study to mathematically investigate the particulate motion of polyethylene pellets on an inclined screening chute using DEM.

The coupled DEM–CFD approach has been used recently to predict the solid interaction with fluids. Li et al. [58] used a 3D coupled DEM–CFD model to study the effects of inlet airflow velocity on the kernels and short straw's longitudinal velocity and vertical height and the cleaning loss in an air-and-screen cleaning device. The rice grain represented by a spheroid and the short straw by a cylinder were generated in EDEM and allowed to fall on an inclined vibrating screen. The CFD portion of the coupling model used the Eulerian–Eulerian model in FLUENT (ANSYS Inc., Canonsburg, PA). The authors used Hertz-Mindlin contact model to simulate particle–particle and particle–screen (wall) collisions. Through the coupled DEM–CFD approach, the authors found that the length of the screen can be shortened if impurity content is lower. The coupled DEM–CFD modeling approach also could be used to improve the design of combine harvesters because the model accurately predicts the particle movement in air.

Impacting of Grain

The impact of grain as it falls on a flat surface influences breakage characteristics, friction, and coefficient of restitution. Wojtkowski et al. [101] proposed that different models have to be used to predict the impact of grain kernels depending on moisture content. The researchers also indicated that to determine a correct contact model, the ratio of the fall time to the rise time (TR) for the contact force–time characteristics should be considered. For TR > 1, the authors recommended the viscoelastic model, whereas the elastoplastic model should be applied for TR < 1.

Another application of DEM in investigating the impact of grain kernel on a surface was reported by Jiang and Qiu [51]. The authors studied the effects of particle mass and the normal contact force between a rice particle and the impact board of an inclined elevator during flow of rice. Rice kernels were represented as ellipsoids composed of seven spheres in EDEM, and celluloid was used as the material for the impact board to study the effect of elevator belt speeds of 0.5 to 1.0 m/s on bulk flow. The authors found that the normal contact force between the flowing rice particles and the impact board increased as the belt speed increased, but belt speed had no effect on tangential contact force. There was a good linear relationship between the rice particle mass and the normal contact force when the rice particle mass was from 0.18 to 0.54 kg. The authors also concluded that the retention stage (i.e., from the time when the normal contact force is <30 % of the maximum normal force to when it became zero) during impact was not beneficial to grain mass flow measurement. Qiu et al. [75] extended this study to include the elevator belt speed of 1.5 m/s and the effect of sliding during impact.

Modeling Confined Grain

Silo Probing

Managing grain quality in a grain handling facility involves sampling the grain from the incoming truck and testing it for quality. To assess quality, incoming bulk grain in trucks or rail cars is probed using mechanical (vacuum) probes. Chung and Ooi [8], using DEM, simulated the penetration of probes in a dense granular medium to evaluate the resistance of granular bulk to the penetration of a moving object and the dynamic force transmission to a contact surface. The setup the authors used was comparable to a confined compression arrangement with a probe to penetrate the bulk granular materials. Glass beads and corn kernels were used in the simulations for comparison purposes. The authors found that the measured and predicted forces fluctuated during penetration into each material. The average trend was repeatable, with corn kernels giving a larger resistance to penetration than glass beads.

Compression

Oil expression by compression is a major processing operation used by grain-based oil industries. Compression of cereal grains is a complicated process to model because it involves changes in density, inner porosity/voids due to oil removal, size, and shape. By incorporating the actual physical changes in the DEM model, Raji and Favier [76] developed a numerical model to predict compression behavior of rapeseeds. The model was based on the actual physical changes during loading of a low-modulus viscoelastic spherical particles and the resulting change in shape that are often neglected during DEM model development. The authors avoided errors in estimating the porosity by compressing beds of rapeseeds before the seedbeds reached the oil point so the void spaces were not filled with oil. The oil point is the state at which the bulk density of the seedbed approaches the seed kernel density. When the threshold pressure is reached, the oil emerges from a seed kernel during mechanical seed-oil expression. DEM predicted the mechanical compression of oilseeds within a standard error of estimate of 0.20, and the predicted stress–strain values were not significantly different from the experimental values. Extending the same modeling approach to canola, soybean, and palm-kernel, Raji and Favier [77] validated their approach of using low-modulus viscoelastic spherical particles for DEM simulations. Raji and Favier [76, 77] concluded that DEM is a useful tool to study the behavior of deformable soft particulates and the outputs from modeling could be used to design and modify oil expression process machinery.

The effects of materials' different shapes during compression were investigated by Chung and Ooi [8, 9], who simulated the confined compression of spherical (glass beads) and non-spherical (corn kernels) particles. The confined compression test simulation was designed to investigate the mechanical response of a granular material under confined compression and the load transfer to the containing walls. The applied vertical load, vertical displacement, vertical force transmitted to the bottom platen, and force transmitted to the walls were measured, and the material properties for silo design, the lateral pressure ratio, and the bulk wall friction were also evaluated. The findings from these studies indicated that accurate representation of particle shape may not be necessary for the prediction of kernels under compression because capturing the key linear dimensions of a particle may be adequate. DEM results indicated that glass spheres, with their tendency to spin more than non-spherical particles, were more sensitive to initial packing arrangement as influenced by the particle generation method. Irregular particles such as corn kernels were not sensitive to particle spacing as affected by the particle generation method. Interparticle friction affected the loading for the containing walls for corn kernels but not for glass beads; this result was attributed to the significant difference in particle stiffness between two particles. Reducing the contact friction allowed more contacts to reach limiting friction for corn, thus resulting in a larger lateral pressure ratio and a smaller load on the bottom platen than for glass beads.

Moisture content is a principal factor that influences the compression, size reduction, and handling behavior of bulk cereal grains. Understanding the effects of moisture on compression through modeling was initiated by Wiącek and Molenda [97]. The authors used EDEM software with rapeseeds represented as single spheres with 1.9 mm diameter and used the physical properties obtained from the literature [96]. The load responses of rapeseed were subjected to uniaxial confined compression quantified at moisture contents of 7.5, 9, and 12 % and were compared with the experimental data. The authors observed that the DEM predicted a softer response for the spherical assembly of rapeseeds compared with the experimental observations. Although the model responses deviated from the actual values, this study illustrated the possibility of using DEM to predict the mechanical behavior of granular materials of biological origin.

Interparticle friction and particle stiffness also influenced the bulk response of grain kernels in DEM simulations under confined compression. Chung and Ooi [10] found that reduction in particle stiffness by a few orders can provide a huge computational advantage, with secondary effects on the load transmission in a quasi-static assembly. The researchers also found that interparticle friction has an effect on the loading of containing walls in simulating confined compression of corn kernels but not of glass beads. For corn kernels, reduced contact friction allowed more contacts to reach limiting friction, resulting in a larger lateral pressure ratio and a smaller load on the bottom of the confined structure.

Modeling the compression of grain has been used to calibrate material properties for DEM simulations [13, 14] and to determine parameter values of cohesionless corn kernels. Coetzee and Els [13] calibrated particle stiffness using confined compression tests (also called oedometer tests) by applying stress to corn kernels along the vertical axis at low compression rates (±2 mm min^{-1}). Numerical simulation of 2D corn kernels indicated that the internal friction angle depended on particle stiffness and the particle friction coefficient. Results of the confined compression test showed that the simulated macro- or bulk stiffness is a linear function of the particle stiffness; thus, particle stiffness can be determined through the confined compression test. This study showed that DEM simulation could enable the determination of particle properties to enhance the understanding of the bulk behavior of cereal grains.

Shear Testing

Discrete element method (DEM) was used to examine the influence of the friction coefficient between two sliding particles on the shear behavior of an assembly of rapeseeds in 2D systems [70]. The authors first measured the interparticle friction coefficients for metal plates, pea, wheat, and rapeseeds. Then, they simulated the direct shear test using 2D DEM models. The authors found that the degree of variation of the coefficient of interparticle friction did not influence the final value of shear strength at steady-state flow; however, the level of standard deviation of the coefficient of interparticle friction markedly influenced the shear path (or shear–strain characteristics) at the initiation of motion.

The effects of moisture content on shear testing were simulated by Sarnavi et al. [82]. They modeled the strength properties of stored wheat kernels at different moisture contents using the Jenike method of direct shear tests [2]. The research group implemented linear and nonlinear models. Three types of particle models were used to create kernels by a multi-sphere approach: (1) spherical, (2) 4 spheres, and (3) 8 spheres. The simulation of bulk behavior was strongly affected by the interparticle interactions and particle shape representation in modeling. Linear models are more capable of representing the variation in strength properties with moisture content than nonlinear models. In general, both linear and nonlinear models have an equal chance of correctly predicting strength properties of the wheat assembly. Spherical grain models best simulated wheat kernels in bulk properties tests. Both the values of internal angle of friction and apparent cohesion have about a 70 % chance of prediction by the DEM model.

Grain Drying

Although grain is considered free-flowing during grain drying, the dense arrangement of the particles inside the grain dryer make them behave like confined particles. Iroba et al. [46, 47] examined the physical phenomena that control particle flow in mixed-flow dryers (MFDs). They investigated the residence time distribution (RTD), particle vertical velocity profiles, and particle trajectories using PFC 2D. Simulation results were validated with experiments using a semi-technical dryer test station with a transparent Plexiglas front wall. Experiments were conducted with moist wheat as a bed material, with an average moisture content of 18 % wet basis (w.b.) and a bulk density of 783 kg m^{-3}. Colored tracer particles were employed in the residence time analysis in the mixed-flow dryer (MFD) to detect particle flow inhomogeneity and design deficit. Simulation results showed that the DEM model adequately predicted particle flow during drying. Through DEM simulation, it was understood that two flow regimes exist in MFDs, the near-wall region and the central region. Particles at the near-wall region had lower particle velocity, whereas the central region had high particle velocity. Wall friction dominated the particle flow near-wall region and had a large effect on the bulk particle movement, whereas particle–particle forces were dominant in the central region. Kernels passing through the MFD have different vertical velocities, thus resulting in different residence times. The presence of two different flow regimes will affect overall dryer capacity and drying efficiency. Kernels flowing at lower velocities may be over-dried, while those moving at high velocities may be under-dried. The authors concluded that the present design of MFDs did not provide adequate cross-mixing, with the effect of the half air ducts dominant on the sidewalls. Consequently, the current design may lead to broad moisture content distribution at the outlet (inhomogeneous drying) with the risk of product quality deterioration during subsequent storage. This study underlined the importance of updated MFD design, such as the need to adjust the size and positions of the half air ducts. Although the 2D DEM model predicted the residence time distributions and the flow patterns, improvements in the approach are needed to map velocity profiles. To depict the grain drying process accurately, numerical simulation should also account for the shrinkage of kernels during drying because this shrinkage alters the particle properties.

To improve the prediction of drying process using DEM, Mellman et al. [64] modeled the effects of design elements and air duct arrangements on MFDs. The authors articulated the same findings as Iroba et al. [46, 47] regarding the RTD in mixed-flow grain dryers. Simulation and experimental results showed that the DEM can adequately predict the main features of particle flow. The half air ducts at the sidewalls obstructed the free flow of grain, resulting in the long tail of the RTD. The studies indicated that the diagonal duct arrangement showed a more even grain moisture and temperature distribution than the horizontal duct arrangement. The airflow distribution in the grain bed in the diagonal arrangement was considered degraded, however, because of the dead zones, which were not flushed by the drying air, in the MFD. The authors concluded that grain bulk and particle moisture content as well as grain temperature distributions fluctuate strongly over the cross section of the dryer, resulting in inhomogeneous drying. The analysis displayed deficits in the present design of MFDs, namely the arrangement and allocation of the air ducts.

Due to variations in grain properties, dryer design, and drying parameters, optimizing dryer design and understanding particle movement inside the dryer is of continued interest in researchers as well as industry. The influence of dryer walls and air ducts on particle velocity distribution in an MFD was investigated by Keppler et al. [53], who modeled the effects of particle–wall friction, air duct apex angle, and wall angle on the vertical direction of particle velocity distribution. The effects of different construction modifications for more even vertical grain particle velocity distribution were analyzed using DEM. The authors found from experiments and simulations that the sidewalls have a strong impact on grain flow, causing segregation; these were similar to the findings by Iroba et al. [46]. Both studies indicated that segregation caused big differences in the residence time of single grain portions and caused uneven drying.

Weigler et al. [94] extended the work of Iroba et al. [46, 47] and Mellman et al. [64] by investigating the particle and airflows in MFDs using DEM and CFD. The particle flow behavior of wheat in the traditional MFD was simulated using PFC 2D. Two different particle representations of wheat, spherical and ellipsoidal, were studied and compared when simulating particle flow. A diagonal air duct arrangement led to dead zones in airflow. Airflow through the grain bed was simulated using CFD, applying the commercial software ANSYS CFX (Release 14.0, ANSYS, Inc., Canonsburg, Penn.). The airflow domain in the dryer apparatus was discretized by generating a finite volume grid employing the software ANSYS ICEM (ANSYS, Inc., Canonsburg, Penn.). The authors found that over- and under-drying occurred in traditionally designed mixed-flow dryers because of unfavorable air duct arrangements; core flow of particles due to the wall friction effect and the half air ducts fixed at the sidewalls, characterized by retarded flow at the dryer walls and a fast flow region in the center; and dead zones in airflow, resulting in uneven airflow, grain flow, and drying conditions over the cross section. They recommended a new dryer design with the airflow distribution adjusted to the particle flow distribution. In regions with higher particle velocities, higher air velocities should be provided. The sidewalls of the dryer should be inclined, and the half air ducts should be removed. Researchers also added that future design development would require a tool that couples the airflow characteristics with the particle flow characteristics, including the heat and mass transfer, such as coupled CFD and DEM simulation.

Weigler et al. [95] used the model they developed for MFDs [94] to study the flow of grain in the process of designing an efficient MFD using PFC 2D. The particle flow was studied by tracing the differently colored kernels through the transparent sidewall of the dryer. Based on the observations, the authors developed a new MFD geometry that results in uniform drying of kernels. The greatest advantage of using DEM modeling techniques in grain drying is the ability to study the grain velocity distribution within the dryer as affected by constructional modifications. This will be of great interest to industry because understanding grain behavior within the dryer allows analysis of drying without requiring an expensive prototype.

A Case Study

In this case study, the commingling of two types of grain in a bucket-type grain elevator boot system is considered based on Boac et al. [5]. Previous research in commercial elevator equipment [43–45] showed large variations between and within facilities for commingling of grain lots, which can greatly increase the number of experiments necessary to make widely applicable inferences. However, DEM was used in this case study to model the commingling in a grain elevator boot system and avoid the time and expense of many more experiments.

A 3D computer-aided design (CAD) drawing (DS SolidWorks Corp., Concord, Mass.) of the pilot-scale bucket elevator leg and boot geometry (model B3, Universal Industries, Inc., Cedar Falls, Iowa) was imported in EDEM 2.3. Grain commingling in the pilot-scale boot was simulated using 3D and quasi-2D DEM models. Simulations were performed at 20 % Rayleigh time step. The Hertz-Mindlin no-slip model [83] was implemented as the contact model for all simulations.

Two types of soybeans with different intrinsic properties were colored red and yellow in the simulation to illustrate their difference. The particle model developed by Boac et al. [4] for soybeans was used. Red soybeans were allowed to flow inside the grain elevator boot geometry. The grain elevator leg (composed of bucket cups) was allowed to run for 15 s of simulation time, until the red soybeans stabilized as the residual grain at the bottom of the boot. With red soybeans as the residual grain, yellow soybeans were generated in the simulation and allowed to accumulate in the left-hand side (LHS) hopper for 15 s before opening the slide gate. Yellow soybeans were then continuously run in the boot for approximately 8 min in simulation time (Fig. 3a).

The same simulation procedure was followed for a quasi-2D DEM model using a periodic boundary and domain width equivalent to 5.6 times the particle diameter (Fig. 3b). The total particle mass of red and yellow soybeans was determined from each bucket cup in all simulations. Predicted average commingling data were computed, plotted at each time interval, and compared with the experimental data. Figure 4 shows that the predicted average commingling from 3D and quasi-2D DEM models of the boot closely matched the experimental data, especially after the flow has stabilized after 100 s. The quasi-2D (5.6d) model reduced simulation run time by 72–74 % compared to the 3D model, with both models being run on the same workstation (Table 4). This case study showed that grain commingling in a bucket elevator boot system can be simulated with both 3D and quasi-2D DEM models, giving results that agreed with the experimental data.

Application of DEM in Other Food Engineering Operations

Postharvest operations in any food engineering applications are complex, and modeling has proved to be effective for prediction, process calculation, and process design purposes. Ho et al. [37] suggested that parallel multiscale modeling, with a complete understanding of the structural aspect of food material, will be the best approach for analyzing and designing food processing systems.

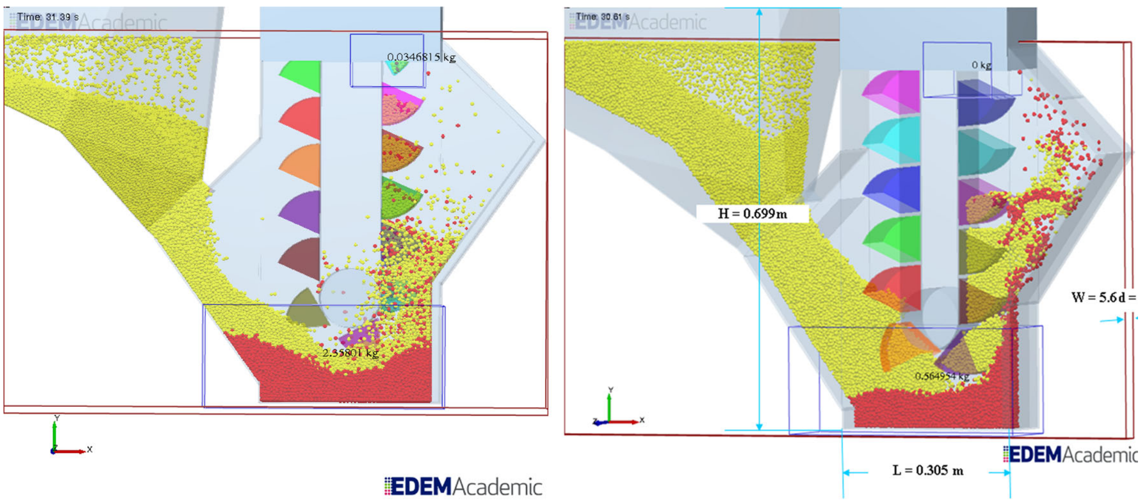

Fig. 3 **a** 3D and **b** quasi-2D DEM models of a pilot-scale boot showing commingling of differently colored soybean particles

Fig. 4 Predicted average commingling from 3D and quasi-2D DEM models

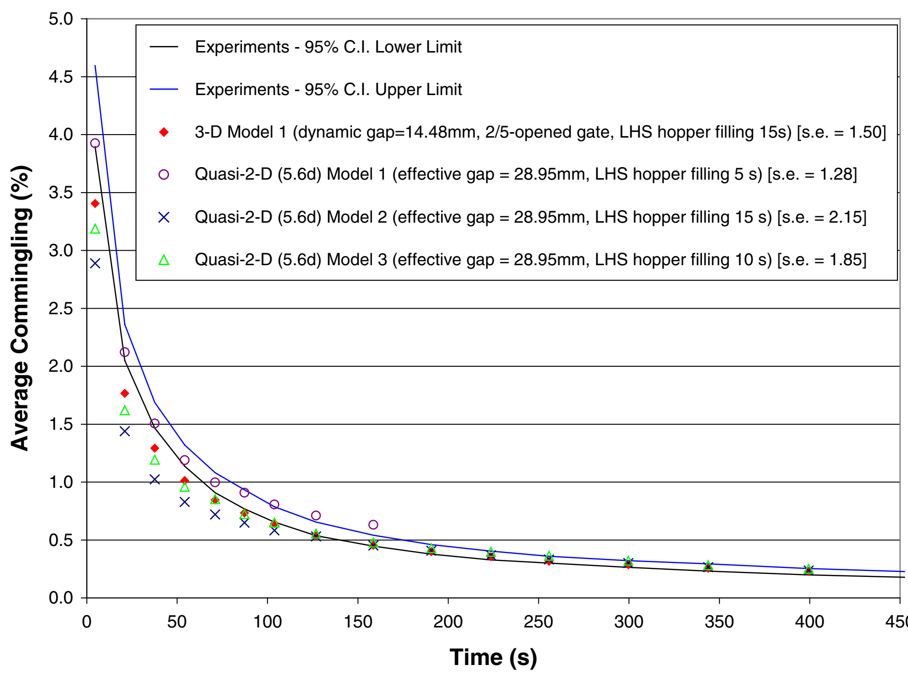

In specific, fresh horticultural crop produce is difficult to model due to their non-uniformity in size and shape and for their higher vulnerability to changes in surface and textural characteristics during handling and transport [1]. Delele et al. [23] developed a combined DEM and computational fluid dynamics (CFD) model to analyze the airflow during cooling through stacks of boxes with horticultural produce. DEM was used to generate random stacking of spheres in the box. Cooling was simulated at different heights of the stack with different diameter spheres. The results indicate that DEM helped identify that random filling has less influence on the air flow resistance than other factors such as confinement ratio, size, porosity, and box vent hole ratio. Through this coupled DEM–CFD approach, the flow profile in individual pores could be analyzed that could not be done through porous media approaches.

Van Zeebroeck et al. [89, 90] applied DEM to study impact damage in apples during transport and handling. The authors used the nonlinear Kuwbara and Kono contact force model, and the parameters were derived experimentally. The model findings were validated using a shaking box approach of vibrating apples in an electro-hydraulic

Table 4 Computational time for 3D and quasi-2D (5.6d) models

Model	Computational time (actual hours per second of simulation time)	Percent difference (from 3D model 1)
3D model 1	0.450	00.00
Quasi-2D model 1	0.118	73.72
Quasi-2D model 2	0.116	74.25
Quasi-2D model 3	0.125	72.24

Simulations were run on a workstation with two Intel Xeon DP Quad-Core W5580 3.2 GHz processors

shaker. Though the authors predicted the bruising damage with reasonable accuracy, multi-impact bruise surfaces and the bruise volume could not be predicted. For vibration damage, the Kuwabara and Kona contact model predicted the condition of apple as influenced by fruit properties and mechanical parameters such as vibration frequency and stack height. Further, the model accurately predicted the existence of damage chains within the apple stack.

Summary and Conclusions

Existing literature that used DEM to simulate postharvest handling and processing, limited to grain and its coproducts, was reviewed. The soft-sphere approach of DEM was commonly used to develop these grain and food processing industry process simulations. The advantage of soft-sphere models was their capability of handling multiple particle contacts, which are of importance when modeling bulk grain systems. The deformations that a grain kernel undergoes during handling and processing were used to calculate elastic, plastic, and frictional forces between particles, and the motion of particles was described by Newton's laws of motion.

Particle models varied with the type of grain. For near-spherical kernels such as soybean and rapeseed, single-sphere particle models predicted particle behavior with greater accuracy. For non-spherical kernels such as rice, wheat, and corn, particle representation using a multi-sphere approach reduced specific simulation errors, but increased simulation time and computational load because of the higher number of contact points requiring force and deformation calculation at each contact point. To avoid this excess computation time problem, most researchers have used single-sphere models and had reasonable success in predictions. Rotation of the single-sphere particles must be properly described, however, because these particles rotate more easily in the simulation than observed in experiments. Thus, the rolling friction coefficient is an important component when using spherical particle models to simulate non-spherical kernels. Depending on the software used, both linear and nonlinear (Hertz-Mindlin) contact models have been used effectively to study grain handling and processing operations.

Discrete element method (DEM) simulations have been used in different grain processing environments, such as those dealing with free-flowing grain and with confined grain, for optimizing processes and to improve equipment design. In general, DEM has adequately simulated post-harvest processing of grain and grain coproducts. In some processes, such as the analysis of discharge from a silo and design of grain dryers, coupling DEM with computational fluid dynamics is recommended for better predictions. Although DEM has been increasingly used to study grain kernel processes, it has not been widely applied. The huge variation in particle characteristics such as size, shape, surface roughness, density, friction coefficients, composition, and other factors could be hindering the use of DEM. Computational cost also limits DEM application; specifically, most of the particles in grain-based food industries are smaller, which leads to higher computation time. Development of precision particle models could help spur adoption of this numerical modeling concept and optimize process and equipment design in the grain handling and processing industry.

Acknowledgments This is contribution No. 14-278-J from the Kansas State University Agricultural Experiment Station.

References

1. Ambaw A, Delele MA, Defraeye T, Ho QT, Opara LU, Nicolai BM, Verboven P (2013) The use of CFD to characterize and design post-harvest storage facilities: past, present and future. Comput Electron Agric 93:184–194
2. ASTM (2006) Standard test method for shear testing of bulk solids using the Jenike shear cell. D6128. American Society for Testing and Materials, West Conshohocken, PA
3. Boac JM (2010) Quality changes, dust generation, and commingling during grain elevator handling. Ph.D. Dissertation. Kansas State University, Manhattan, Kansas
4. Boac JM, Casada ME, Maghirang RG, Harner JP (2010) Material and interaction properties of selected grains and oilseeds for modeling discrete particles. Trans ASABE 53(4):1201–1216
5. Boac JM, Casada ME, Maghirang RG, Harner JP (2012) 3-D and quasi-2-D discrete element modeling of grain commingling in a bucket elevator boot system. Trans ASABE 55(2):659–672
6. Boukouvala F, Gao Y, Muzzio F, Ierapetritou MG (2013) Reduced-order discreter element method modeling. Chem Eng Sci 95:12–26
7. Campbell CS (2006) Granular material flows—an overview. Powder Technol 162:208–229

8. Chung YC, Ooi JY (2006) Confined compression and rod penetration of a dense granular medium: discrete element modeling and validation. In: Wu W, Yu HS (eds) Modern trends in geomechanics. Springer, Berlin, pp 223–239
9. Chung YC, Ooi JY (2008) Influence of discrete element model parameters on bulk behavior of a granular solid under confined compression. Part Sci Technol 26(1):83–96
10. Chung YC, Ooi JY (2008) A study of influence of gravity on bulk behaviour of particulate solid. Particuology 6(6):467–474
11. Chung YC, Ooi JY, Favier JF (2004) Measurement of mechanical properties of agricultural grains for DE models. In: *17th ASCE Engineering Mechanics Conference*. American Society of Civil Engineers, Newark, Delaware
12. Clementson CL (2010) The granulometric heterogeneity of distillers dried grains with solubles (DDGS) and its effect on the bulk physical and chemical properties. Ph.D. Thesis. Purdue University, West Lafayette, Indiana
13. Coetzee CJ, Els DNJ (2009) Calibration of discrete element parameters and the modelling of silo discharge and bucket filling. Comput Electron Agric 65(2):198–212
14. Coetzee CJ, Els DNJ (2009) Calibration of granular material parameters for DEM modelling and numerical verification by blade-granular material interaction. J Terrramech 46(1):15–26
15. Coetzee CJ, Els DNJ (2009) The numerical modelling of excavator bucket filling using DEM. J Terrramech 46(5):217–227
16. Coetzee CJ, Els DNJ, Dymond GF (2010) Discrete element parameter calibration and the modelling of dragline bucket filling. J Terrramech 47(1):33–44
17. Cundall PA (1988) Computer simulations of dense sphere assemblies. In: Satake M, Jenkins JT (eds) Micromechanics of granular materials. Elsevier, Amsterdam, pp 113–123
18. Cundall PA (1988) Formulation of a three-dimensional distinct element method. Part I A: scheme to detect and represent contacts in a system composed of many polyhedral blocks. International Journal of Rock Mechanics and Mining Sciences and Geomechanics Abstracts 25(3):107–116
19. Cundall PA, Hart RD (1989) Numerical modeling of discontinua. In: Mustoe GGW (ed) Proceedings of the 1st U.S. conference on discrete element methods. CSM Press, Golden
20. Cundall PA, Strack ODL (1979) A discrete numerical model for granular assemblies. Geotechnique 29(1):47–65
21. de Bruyn JR (2012) When does a granular material behave like a continuum fluid? J Fluid Mech 704:1–4
22. Delaney G, Inagaki S, Aste T (2007) Fine tuning DEM simulations to perform virtual experiments with three dimensional granular packings. In: Aste Y, Di Matteo T, Tordesillas A (eds) Granular and complex materials. World Scientific, Singapore, pp 141–168
23. Delele MA, Tijskens E, Atalay YT, Ho QT, Ramon H, Nicolai BM, Verboven P (2008) Combined discrete element and CFD modelling of airflow through random stacking of horticultural products in vented boxes. J Food Eng 89(1):33–41
24. Dewicki G (2003) Bulk material handling and processing—numerical techniques and simulation of granular material. Bulk Solids Handling: International Journal of Storing and Handling Bulk Materials 23(2):110–113
25. Di Renzo A, Di Maio FP (2004) Comparison of contact-force models for the simulation of collisions in DEM-based granular flow codes. Chem Eng Sci 59(3):525–541
26. Di Renzo A, Di Maio FP (2005) An improved integral non-linear model for the contact of particles in distinct element simulations. Chem Eng Sci 60(5):1303–1312
27. FAO (2013) Zae mays L. Food and Agriculture Organization of the United Nations. FAO, Rome
28. Favier JF, Abbaspour-Fard MH, Kremmer M, Raji AO (1999) Shape representation of axi-symmetrical, non-spherical particles in discrete element simulation using multi-element model particles. Eng Comput 16(4):467–480
29. Ferellec JF, McDowell GR (2010) A method to model realistic particle shape and inertia in DEM. Granular Matter 12(5):459–467
30. Fortin J, Millet O, de Saxce G (2004) Numerical simulation of granular materials by an improved discrete element method. Int J Numer Meth Eng 62:639–663
31. Ghaboussi J, Barbosa R (1990) Three-dimensional discrete element method for granular materials. Int J Numer Anal Meth Geomech 14(7):451–472
32. González-Montellano C, Ramirez A, Gallego E, Ayuga F (2011) Validation and experimental calibration of 3D discrete element models for the simulation of the discharge flow in silos. Chem Eng Sci 66(21):5116–5126
33. González-Montellano C, Ramirez A, Fuentes JM, Ayuga F (2012) Numerical effects derived from *en masse* filling of agricultural silos in DEM simulations. Comput Electron Agric 81:113–123
34. González-Montellano C, Gallego E, Ramirez-Gomez A, Ayuga F (2012) Three dimensional discrete element models for simulating the filling and emptying of silos: analysis of numerical results. Comput Chem Eng 40:22–32
35. González-Montellano C, Fuentes JM, Ayuga- Tellez E, Ayuga F (2012) Determination of the mechanical properties of maize grains and olives required for use in DEM simulations. J Food Eng 111(4):553–562
36. Hart R, Cundall PA, Lemos J (1988) Formulation of a three-dimensional, distinct element method, Part II: mechanical calculations for motion and interaction of a system composed of many polyhedral blocks. Int J Rock Mech Min Sci Geomech Abs 25(3):117–125
37. Ho QT, Carmeliet J, Datta AK, Defraeye T, Delele MA, Herremans E, Opara L, Ramon H, Tijskens E, Sman Rvd, Liedekerke PV, Verboven P, Nicolai BM (2013) Multiscale modeling in food engineering. J Food Eng 114:279–291
38. Hocking G (1992) The discrete element method of analysis of fragmentation of discontinua. Engineering Computation 9(2):145–155
39. Hogue C (1998) Shape representation and contact detection for discrete element simulations of arbitrary geometries. Eng Comput 15(3):374–390
40. Hoomans BPB, Kuipers JAM, Briels WJ, Van Swaaij WPM (1996) Discrete particle simulation of bubble and slug formation in a two-dimensional gas-fluidized bed: a hard-sphere approach. Chem Eng Sci 51(1):99–118
41. Hustrulid AI (1998) Transfer station analysis. Paper presented at the 1998 SME Annual Meeting, Orlando, Florida
42. Hustrulid AI, Mustoe GGW (1996) Engineering analysis of transfer points using discrete element analysis. Paper presented at the 1996 SME Annual Meeting, Phoenix, Arizona
43. Ingles MEA (2005) Identity preservation of grain in elevators. Unpublished PhD dissertation. Kansas State University Department of Biological and Agricultural Engineering, Manhattan, Kansas
44. Ingles MEA, Casada ME, Maghirang RG (2003) Handling effects on commingling and residual grain in an elevator. Transactions of the ASAE 46(6):1625–1631
45. Ingles MEA, Casada ME, Maghirang RG, Herrman TJ, Harner JP III (2006) Effects of grain-receiving system on commingling in a country elevator. Appl Eng Agric 22(5):713–721
46. Iroba KL, Mellman J, Weigler F, Metzger T, Tsotsas E (2011) Particle velocity profiles and residence time distribution in mixed-flow grain dryers. Granular Matter 13(2):159–168
47. Iroba KL, Weigler F, Mellman J, Metzger T, Tsotsas E (2011) Residence time distribution in mixed-flow grain dryers. Drying Technol 29(11):1252–1266

48. Isik E (2007) Some engineering properties of soybean grains. Am J Food Technol 2:115–125
49. Itasca (2008) PFC3D Particle flow code in 3 dimensions: Theory and background. Itasca Consulting Group, Minneapolis, Minn. 40 p
50. Jean M, Moreau JJ (1991) Dynamics of elastic or rigid bodies with frictional contact: numerical methods. Publications du L.M.A. 124:9–29
51. Jiang G, Qiu B (2011) Discrete element method simulation of impact-based measurement of grain mass flow. In Proceedings of the 2011 international conference on computer distributed control and intelligent environmental monitoring 5747847: 419–422
52. Kačianauskas R, Maknickas A, Kačeniauskas A, Markauskas D, Balevičius R (2010) Parallel discrete element simulation of poly-dispersed granular material. Adv Eng Softw 41(1):52–63
53. Keppler I, Kocsis L, Oldal I, Farkas I, Csatar A (2012) Grain velocity distribution in a mixed flow dryer. Adv Powder Technol 23(6):824–832
54. Kuwabara G, Kono K (1987) Restitution coefficient in a collision between two spheres. Jpn J Appl Phys 26(8):1230–1233
55. Li J, Webb C, Pandiella SS, Campbell GM (2002) A numerical simulation of separation of crop seeds by screening—effect of particle bed depth. Food Bioproducts Process Trans Inst Chem Eng Part C 80(2):109–117
56. Li J, Webb C, Pandiella SS, Campbell GM (2003) Discrete particle motion on sieves: a numerical study using the DEM simulation. Powder Technol 133(1–3):190–202
57. Li Y, Xu Y, Thornton C (2005) A comparison of discrete element simulations and experiments for 'sandpiles' composed of spherical particles. Powder Technol 160(3):219–228
58. Li H, Li Y, Gao F, Zhao Z, Xu L (2012) CFD-DEM simulation of material motion in air-and-screen cleaning device. Comput Electron Agric 88:111–119
59. Lin X, Ng TT (1997) A three-dimensional discrete element model using arrays of ellipsoids. Geotechnique 47(2):319–329
60. LoCurto GJ, Zhang X, Zarikov V, Bucklin RA, Vu-Quoc L, Hanes DM, Walton OR (1997) Soybean impacts: experiments and dynamic simulations. Trans ASAE 40(3):789–794
61. Lu M, McDowell GR (2007) The importance of modelling ballast particle shape in the discrete element method. Granular Matter 9(1–2):69–80
62. Markauskas D, Kačianauskas R (2011) Investigation of rice grain flow by multi-sphere particle model with rolling resistance. Granular Matter 13(2):143–148
63. Markauskas D, Kačianauskas R, Džiugys A, Navakas R (2010) Investigation of adequacy of multi-sphere approximation of elliptical particles for DEM simulations. Granular Matter 12(1):107–123
64. Mellman J, Iroba KL, Metzger T, Tsotsas E, Mészáros C, Farkas I (2011) Moisture content and residence time distributions in mixed-flow grain dryers. Biosyst Eng 109(4):297–307
65. Metzger MJ, Glasser BJ (2013) Simulation of the breakage of bonded agglomerates in a ball mill. Powder Technol 237: 286–302
66. Miller GF, Pursey H (1955) On the partition of energy between elastic waves in a semi-infinite solid. Proc R Soc Lond A 233(1192):55–69
67. Mindlin RD (1949) Compliance of elastic bodies in contact. J Appl Mech 16:259–268
68. Mindlin RD, Deresiewicz H (1953) Elastic spheres in contact under varying oblique forces. Trans ASME Series E J Appl Mech 20:327–344
69. Mishra BK (2003) A review of computer simulation of tumbling mills by the discrete element method: part I—contact mechanics. Int J Miner Process 71(1–4):73–93
70. Molenda M, Horabik J, Lukaszuk J, Wiącek J (2011) Variability of intergranular friction and its role in DEM simulation of direct shear of an assembly of rapeseeds. Int Agrophys 25(4):361–368
71. O'Sullivan C (2011) Particle-based discrete element modeling: geomechanics perspective. Int J Geomechan 11(6):449–464
72. O'Sullivan C (2011) Particulate discrete element modelling: a geomechanics perspective. Spon Press, New York
73. Parafiniuk P, Molenda M, Horabik J (2013) Discharge of rapeseeds from a model silo: physical testing and discrete element method simulations. Comput Electron Agric 97:40–46
74. Potyondy DO, Cundall PA (2004) A bonded-particle model for rock. Int J Rock Mech Min Sci 41(8):1329–1364
75. Qiu B, Jiang G, Yang N, Guan X, Xie J, Li Y (2012) Discrete element method analysis of impact action between rice particles and impact-board. Trans Chin Soc Agric Eng 28(3):44–49 (Chinese)
76. Raji AO, Favier JF (2004) Model for the deformation in agricultural and food particulate materials under bulk compressive loading using discrete element method. Part I: theory, model development and validation. J Food Eng 64(3):359–371
77. Raji AO, Favier JF (2004) Model for the deformation in agricultural and food particulate materials under bulk compressive loading using discrete element method. Part II: compression of oilseeds. J Food Eng 64(3):373–380
78. Remy B, Khinast JG, Glasser BJ (2009) Discrete element simulation of free-flowing grains in a four-bladed mixer. AIChE J 55(8):2035–2048
79. Rowlands, JC (1991) Dragline bucket filling. Ph.D. Thesis. University of Queensland, Queensland, Australia
80. Sakaguchi E, Kawakami S, Tobita F (1994) Simulation on flowing phenomena of grains by distinct element method. Eur. Ag. Eng. Paper No. 94-G-025. Ag. Eng.'94, Milano
81. Sakaguchi E, Suzuki M, Favier JF, Kawakami S (2001) Numerical simulation of the shaking separation of paddy and brown rice using the discrete element method. J Agric Eng Res 79(3):307–315
82. Sarnavi HJ, Mohammadi AN, Motlagh AM, Didar AR (2013) DEM model of wheat grains in storage considering the effect of moisture content in direct shear test. Res J Appl Sci Eng Technol 5(3):829–841
83. DEM Solutions (2013) EDEM 2.5 User Guide. DEM Solutions, Ltd., Edinburgh, UK
84. Theuerkauf J, Dhodapkar S, Jacob K (2007) Modeling granular flow using discrete element method—from theory to practice. Chem Eng 114(4):39–46
85. Thornton C, Ning Z (1998) A theoretical model for the stick/bounce behaviour of adhesive, elastic-plastic spheres. Powder Technol 99(2):154–162
86. Ting JM, Khwaja M, Meachum L, Rowell JD (1993) An ellipse based discrete element model for granular materials. Int J Numer Anal Meth Geomech 17(9):603–623
87. Tsuji Y, Tanaka T, Ishida T (1992) Lagrangian numerical simulation of plug flow of cohesionless particles in a horizontal pipe. Powder Technol 71(3):239–250
88. USDA ERS (2013) Oil Crops Yearbook. U.S. Department of Agriculture Economic Research Service, Washington, D.C. http://www.ers.usda.gov/data-products/oil-crops-yearbook.aspx#.UupiItJdUS4
89. Van Zeebroeck M, Tijskens E, Dintwa E, Kafashan J, Loodts J, De Baerdemaeker J, Ramon H (2006) The discrete element method (DEM) to simulate fruit impact damage during transport and handling: model building and validation of DEM to predict bruise damage of apples. Postharvest Biol Technol 41:85–91
90. Van Zeebroeck M, Tijskens E, Dintwa E, Kafashan J, Loodts J, De Baerdemaeker J, Ramon H (2006) The discrete element method (DEM) to simulate fruit impact damage during transport

and handling: case study of vibration damage during apple bulk transport. Postharvest Biol Technol 41:92–100
91. Vu-Quoc L, Zhang X, Walton OR (2000) A 3-D discrete-element method for dry granular flows of ellipsoidal particles. Comput Methods Appl Mech Eng 187(3–4):483–528
92. Walton OR (1983) Particle—dynamics calculations of shear flow. In: Jenkins JT, Satake M (eds) Micromechanics of granular materials: new models and constitutive relations. Elsevier, Amsterdam, pp 327–338
93. Wassgren CR (1997) Vibration of granular materials. Ph.D. Thesis. California Institute of Technology, Pasadena, California
94. Weigler F, Scaar H, Mellmann J (2012) Investigation of particle and air flows in a mixed-flow dryer. Drying Technol 30(15): 1730–1741
95. Weigler F, Mellmann J, Franke G, Scaar H (2013) Experimental studies on a newly developed mixed-flow dryer. Drying Technol 31:1736–1743
96. Wiącek J (2008) Discrete element modeling of quasi-static effects in grain assemblies. PhD Thesis, Institute of Agrophysics, PAS, Lublin
97. Wiącek J, Molenda M (2011) Moisture-dependent physical properties of rapeseed—experimental and DEM modeling. International Agrophysics 25(1):59–65
98. Wightman C, Moakher M, Muzzio FJ, Walton OR (1998) Simulation of flow and mixing of particles in a rotating and rocking cylinder. J Am Inst Chem Eng 44(6):1266–1276
99. Williams JR, Pentland AP (1989) Superquadrics and modal dynamics for discrete elements in concurrent design. In: 1st US conference on the discrete element method, Golden
100. Williams JR, Hocking G, Mustoe GGW (1985) The theoretical basis of the discrete element method. NUMETA '85 Numerical Methods in Engineering, Theory and Applications. Balkema, Rotterdam
101. Wojtkowski M, Pecen J, Horabik J, Molenda M (2010) Rapeseed impact against a flat surface: physical testing and DEM simulation with two contact models. Powder Technol 198(1): 61–68
102. Zhou YC, Xu BH, Yu AB, Zulli P (2001) Numerical investigation of the angle of repose of monosized spheres. Phys Rev E Stat Nonlin, Soft Matter Phys 64(2):213011–213018
103. Zhu HP, Zhou ZY, Yang RY, Yu AB (2007) Discrete particle simulation of particulate systems: theoretical developments. Chem Eng Sci 62(13):3378–3396